

Search for Double Beta Decay in $\text{Nd}^{150}\dagger$

LARRY V. EAST*

Case Institute of Technology, Cleveland, Ohio

(Received 6 April 1966)

Lower limits were obtained for the half-life of the double beta decay of Nd^{150} using thin plastic scintillation detectors surrounded by a large liquid scintillation anticoincidence shield. The experiment was performed 585 m underground in the relatively low-radioactive-background environment of a salt mine. The observed count rates are consistent with a lower limit of 3×10^{17} years for the half-life of the decay $\text{Nd}^{150} \rightarrow \text{Sm}^{150} + 2e^- + 2\bar{\nu}_e$, and 5×10^{18} years for the decay $\text{Nd}^{150} \rightarrow \text{Sm}^{150} + 2e^-$. A lower limit of $\sim 10^{17}$ years was also obtained for the single beta decay $\text{Nd}^{150} \rightarrow \text{Pm}^{150} + e^- + \bar{\nu}_e$.

1. INTRODUCTION

ATTEMPTS to observe double beta decay have been made by many experimenters using a variety of techniques since the original work of Fireman in 1948.¹ Several experiments appeared to obtain positive identification of double beta decay only to have later experiments fail to confirm their results, with one possible exception,² the decay $\text{Te}^{150} \rightarrow \text{Xe}^{150}$. Using mass spectrographic techniques, Inghram and Reynolds,³ and more recently Takaoka and Ogata,⁴ have obtained a half-life for this decay consistent with recent theoretical estimates.⁵ However, no experiment has yet been able to detect unambiguously the simultaneous emission of two electrons from a double beta-decay source.

Prior to 1957, interest in double-beta-decay experiments was given impetus by arguments which related the decay rate to the "type" of neutrino involved.⁶ If the neutrino were a Majorana particle ($\nu \equiv \bar{\nu}$), then a decay of the type

$$Z^A \rightarrow (Z \pm 2)^A + 2e^\mp \quad (1)$$

could occur, resulting in nonconservation of total lepton number. If, on the other hand, the neutrino were a Dirac particle, then double beta decay must occur with the emission of two neutrinos (or antineutrinos) with at least a five order of magnitude decrease in the decay rate. However, changes in weak-interaction theory brought about by the discovery of parity nonconservation indicate that double beta decay without the emis-

sion of neutrinos is ruled out unless there is a small deviation from two-component neutrino coupling in the nucleon-lepton interaction (as would be the case, for example, if $m_\nu \neq 0$) along with the nonconservation of total lepton number. On the other hand, the absence of neutrinoless double beta decay does not guarantee lepton conservation as was once thought.^{5,7}

The neutrinoless mode of decay is considerably easier to look for experimentally, since all of the decay energy would be shared by the two electrons rather than by the two electrons and two neutrinos. Therefore, the sum of the electron kinetic energies would have a unique value and the decay would be more easily recognized in the presence of background. The earlier energy-sensitive counter experiments looked only for the neutrinoless mode of decay. Two recent experiments that were sensitive to the two-neutrino mode of decay from Ca^{48} , however, failed to yield positive results.^{8,9} An earlier experiment using Nd^{150} was sensitive only to the neutrinoless mode of decay.¹⁰ Since the experimental limits obtained for the half-life for the neutrinoless mode were much greater than that predicted by theory, the present experiment was designed primarily to search for the two-neutrino decay mode of Nd^{150} decay although it was sensitive to the neutrinoless mode as well.

A summary of recent experimental and theoretical results obtained for Ca^{48} and Nd^{150} , the two most promising double beta decay candidates, is given in Table I.

The present investigation made use of a much larger amount of separated isotope ($\sim 43\text{g}$) than had been available in the past, allowing a shorter run time than would otherwise have been possible. The equipment consisted of a main detector constructed of thin plastic scintillators placed inside a large anticoincidence shield containing approximately 500 gal of liquid scintillator. The detectors were located 585 m below ground ($\sim 1300\text{-m}$ water equivalent) in a salt mine, resulting in a reduction in low-energy γ -ray background by a factor

⁷ E. Greuling and R. C. Whitten, *Ann. Phys.* **11**, 510 (1960).

⁸ E. der Mateosian and M. Goldhaber, *Phys. Rev.* **146**, 810 (1966).

⁹ M. H. Shapiro, S. Frankel, S. Koicki, W. Whales, and G. T. Wood, *Bull. Am. Phys. Soc.* **10**, 424 (1965); M. H. Shapiro, American Physical Society Meeting, New York, June 1965.

¹⁰ C. L. Cowan, Jr., F. B. Harrison, L. M. Langer, and F. Reines, *Nuovo Cimento* **3**, 649 (1956); C. L. Cowan, Jr., and F. Reines, *Phys. Rev.* **106**, 825 (1957).

[†] Work supported by the U. S. Atomic Energy Commission. Preliminary results of this work were presented at the 1965 Spring APS Meeting in Washington, D. C. [L. V. East, T. L. Jenkins, and F. Reines, *Bull. Am. Phys. Soc.* **10**, 442 (1965)].

* Present address: Air Force Weapons Laboratory, Kirtland Air Force Base, Albuquerque, New Mexico. This paper is based on a thesis submitted in partial fulfillment of the requirements for the degree of Doctor of Philosophy at Case Institute of Technology.

¹ E. L. Fireman, *Phys. Rev.* **74**, 1238 (1948); **75**, 323 (1949).

² For a discussion of double beta decay experiments prior to 1957, see James S. Allen, *The Neutrino* (Princeton University Press, Princeton, New Jersey, 1958), Chap. 6.

³ M. G. Inghram and J. H. Reynolds, *Phys. Rev.* **76**, 1265 (1949); **78**, 822 (1950). R. J. Hayden and M. G. Inghram, *Natl. Bur. Std. (U.S.) Circ.* **522**, 189 (1953).

⁴ N. Takaoka and K. Ogata, *Z. Naturforschung* **21a**, 84 (1966).

⁵ H. Primakoff and S. P. Rosen, *Rept. Progr. Phys.* **22**, 121 (1959); in *Alpha-, Beta-, and Gamma-Ray Spectroscopy*, edited by K. Siegbahn (North-Holland Publishing Company, Amsterdam, 1965), Chap. XXIV, Sec. (J).

⁶ W. H. Furry, *Phys. Rev.* **56**, 1184 (1939).

TABLE I. Double beta decay of Nd^{150} and Ca^{48} .

Decay	Half-life (yrs)		Method of determination	Reference
	Neutrinoless	Two neutrinos		
$\text{Ca}^{48} \rightarrow \text{Ti}^{48}$	$3 \times 10^{15 \pm 2}$	$1 \times 10^{21 \pm 2}$	Theoretical	a
	...	$1 \times 10^{19 \pm 1}$	Theoretical	b
	$> 5 \times 10^{19}$	$> 3 \times 10^{18}$	Experimental	c
	$> 2 \times 10^{20}$	$> 5 \times 10^{18}$	Experimental	d
	$> 4 \times 10^{18}$	$> 2 \times 10^{18}$	Experimental	e
$\text{Nd}^{150} \rightarrow \text{Sm}^{150}$	$3 \times 10^{15 \pm 2}$	$2 \times 10^{21 \pm 2}$	Theoretical	f
	...	$2 \times 10^{19 \pm 1}$	Theoretical	f
	$> 3 \times 10^{18}$...	Experimental	g
	$> 5 \times 10^{18}$	$> 3 \times 10^{17}$	Experimental	Present work

^a See Ref. 5.

^b See Ref. 7.

^c V. R. Lazarenko, and S. Yu. Luk'yanov, Zh. Eksperim. i Teor. Fiz. 49, 751 (1965) [English transl. Soviet Phys.—JETP 22, 521 (1966)].

^d See Ref. 8.

^e See Ref. 9.

^f Results given in Refs. 5 and 7, respectively, were re-evaluated using the more recent value of 3.4 MeV in place of 3.7 MeV as the decay energy of $\text{Nd}^{150} \rightarrow \text{Sm}^{150}$. (See Ref. 24.)

^g See Ref. 10.

of 20 or more and in cosmic-ray-induced background by a factor of $\sim 4 \times 10^4$ over that at ground level.

2. EQUIPMENT DESIGN AND OPERATION

Main Detector

The main detector assembly is shown schematically in Fig. 1. It was constructed from three sheets of Pilot "B" plastic scintillator,¹¹ two sheets $41.6 \text{ cm} \times 41.9 \text{ cm} \times 0.33 \text{ cm}$ and one sheet $41.6 \text{ cm} \times 41.9 \text{ cm} \times 0.46 \text{ cm}$. The scintillator thicknesses were chosen to reduce the background due to γ rays while still maintaining a reasonable detection efficiency for double beta decay events. The three sheets were held in a Plexiglas frame one above the other, with the 0.46-cm sheet in the center. E.M.I. type 6097S 2-in. photomultiplier tubes viewed the scintillators through plastic light pipes of the type described by Gorenstein and Luckey.¹² The top and bottom scintillator sheets were viewed by one phototube each, and the center sheet was viewed by two phototubes. The Nd sources were located between the scintillator sheets. Extensions to the Plexiglas frame holding the sheets held the light pipes in place. The detector assembly was sealed in a liquid tight package with 5-mil Mylar covers and placed horizontally in the center

of the anticoincidence tank. The Mylar covers were pressed directly against the upper and lower sheets of plastic scintillator resulting in the minimum possible amount of inert material located between the plastic and liquid scintillators.

Energy calibration of the main detector was accomplished by observing the peaks in the pulse-height spectra produced by relativistic cosmic ray muons passing through the plastic scintillators. In order to determine the "effective" energy loss of cosmic ray muons per unit thickness of Pilot "B" scintillator, the pulse-height spectra produced in various thicknesses of scintillator were compared with the spectra produced by the 0.625-MeV internal conversion electrons from a Cs^{137} source. The results of these measurements yielded an effective dE/dx of $(1.80 \pm 0.05) \text{ MeV/g cm}^2$, in agreement with the measured energy loss of minimum ionizing muons in plastic scintillator.¹³

Uniformity of response of the plastic scintillators was determined before assembly of the complete detector by placing a small Bi^{207} source at various positions on the scintillator sheets and observing the 0.97-MeV internal conversion line on a 400-channel pulse-height analyzer (PHA). For the 0.33-cm-thick scintillator sheets (counters A and C), the pulse height remained constant within $\pm 12\%$ as the source was moved to various positions over the sheets. For the 0.46-cm-thick detector, the pulse height from each of the two phototubes viewing the scintillator was found to shift about 30% as the source was moved from the center to a side edge of the sheet, and about 15% as it was moved from the edge viewed by a light pipe to the center of the sheet. The uniformity of response of this detector was improved considerably by summing the pulses from the two phototubes, but the response near the edges of the scintillator was still poorer than for the 0.33-cm-thick counters.

The over-all response of each scintillator was obtained from the cosmic-ray pulse-height spectra pro-

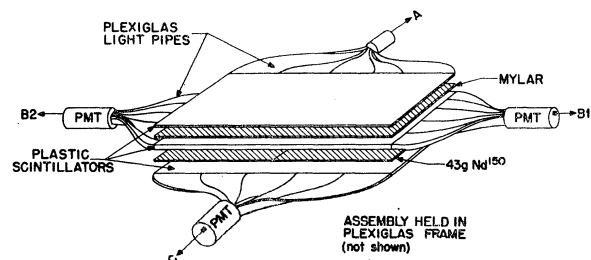


FIG. 1. Main detector assembly.

¹¹ Pilot Chemicals, Inc., Watertown, Massachusetts.

¹² P. Gorenstein and D. Luckey, Rev. Sci. Instr. 34, 196 (1963); see also P. A. Piroué, Natl. Acad. Sci.—Natl. Res. Council Publ. 1184, 46 (1964).

¹³ A. Crispin and P. J. Hayman, Proc. Phys. Soc. (London) 83, 1050 (1964).

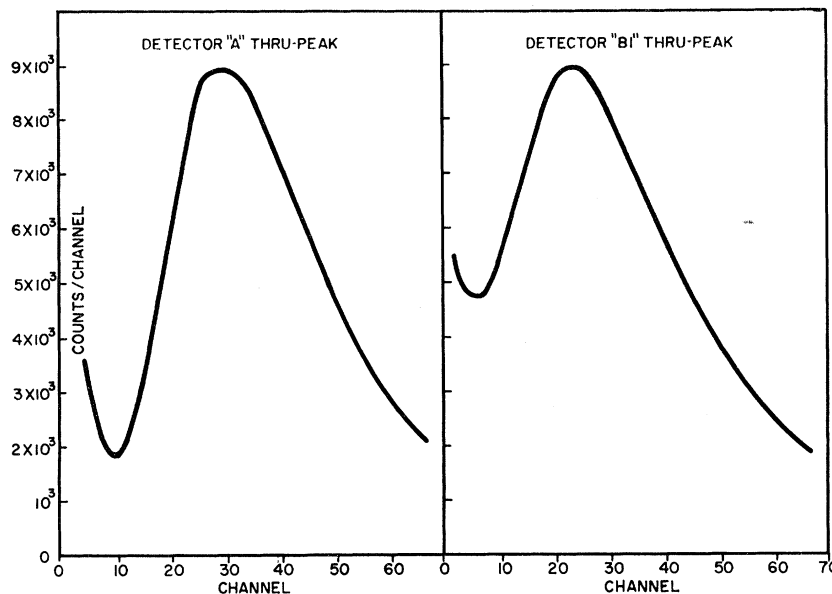


FIG. 2. Main detector cosmic-ray pulse-height spectra.

duced by gating the PHA from the scintillator directly above or below the one being analyzed. The energy-resolution as determined from the half-width at half-maximum on the low-energy side of the peak was found to be 32% for scintillators *A* and *C*, and about 50% from each of the two phototubes viewing scintillator *B*. Typical spectra are shown in Fig. 2.

When the detector was located underground, it was not practical to obtain the cosmic-ray spectra on a PHA because of the long run times required. Spectra were therefore obtained by photographing the detector pulses displayed on an oscilloscope whenever an energy deposit of 100 MeV or more occurred in the anticoincidence detector. The film was then scanned for events in which a pulse appeared from each of the four detector outputs. The spectra obtained in this way were in good agreement with the spectra obtained above ground. Cosmic ray spectra were obtained underground at approximately two-week intervals while the experiment was in progress. A check of the detector stability was made during the intervening time by means of a pulsed light source¹⁴ mounted inside the detector assembly. No change greater than that expected from the jitter of the light source was observed from day to day in the pulse heights from the detector outputs.

Anticoincidence Guard

The anticoincidence guard was a cylindrical steel tank 112 cm high and 152 cm in diameter, filled with liquid scintillator. The scintillator was viewed by 100 5-in. photomultiplier tubes through plastic windows arranged symmetrically around the side of the tank, resulting in about 12.5% of the tank area being

covered by photocathodes. High voltage was supplied to all tubes from a common power supply. The liquid scintillator consisted of 2,5-diphenyl oxazole and dimethyl-POPOP dissolved in a commercial solvent. Individual tubes were adjusted to approximately the same gain by means of resistors added in series with the high voltage leads. Signal outputs from all photomulti-

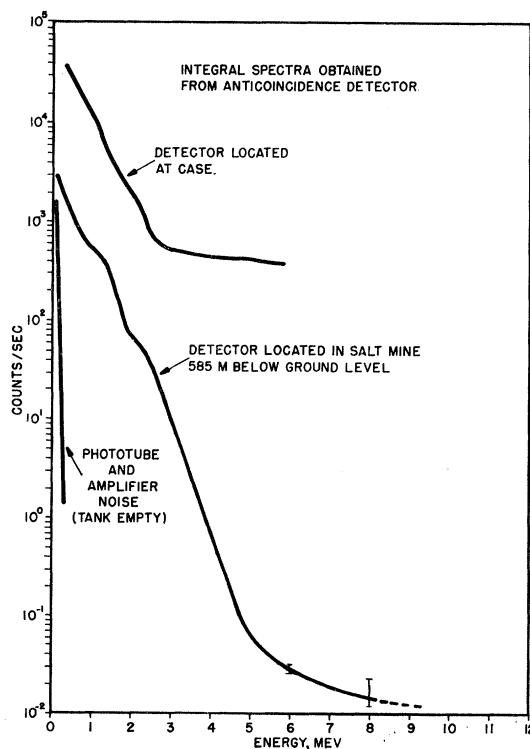


FIG. 3. Integral count rate spectra from the anticoincidence detector.

¹⁴ F. A. Kirsten, IRE Trans. Nucl. Sci. NS-9, 333 (1962).

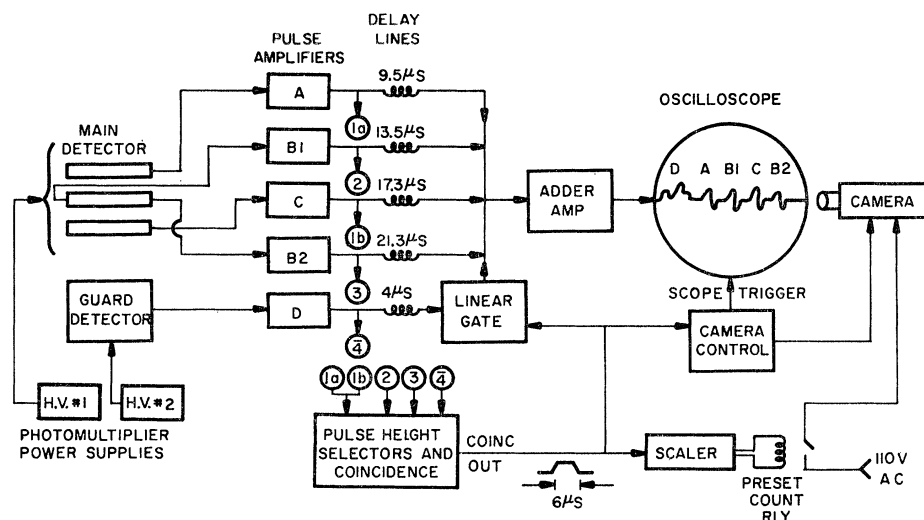


FIG. 4. Block diagram of the data-recording system.

pliers were connected to a common shielded signal line and fed into a charge-sensitive preamplifier.

Energy calibration of the anticoincidence detector was accomplished by use of low-intensity γ -ray sources suspended in the liquid scintillator and with the natural K^{40} background present in the mine. The full width at half-maximum energy resolution of the detector was found to be 29% at 0.66 MeV and 15% at 2.76 MeV.

The integral count rate spectrum obtained from the detector prior to moving it underground is compared to the spectrum obtained underground in Fig. 3. Also shown in the figure is the noise spectrum obtained by operating the detector underground before it was filled with liquid scintillator. The noise did not add materially to the count rate underground at energies greater than about 50 keV.

When the detector was underground, two energy peaks were quite evident in the differential pulse-height spectrum: one at 1.46 MeV due to K^{40} and one at 2.6 MeV due to ThC'' (Tl^{208}). The prominent K^{40} peak is the result of the potassium content of the salt in the mine¹⁵ and of the glass in the phototubes. The ThC'' can be attributed to the steel used to construct the detector tank.¹⁶

Stability of the anticoincidence detector was checked before and after each data run by observing the position of the K^{40} background peak on a pulse-height analyzer relative to a precision pulse generator.

Data-Collection System

A block diagram of the electronics associated with the detectors is shown in Fig. 4. The linear amplifiers were ORNL A-8 type with double delay-line pulse shaping.¹⁷

¹⁵ The potassium content of the salt was measured by H. A. May of the Argonne National Laboratory and found to be ~ 70 ppm.

¹⁶ J. A. DeVoe, Natl. Acad. Sci.—Natl. Res. Council Publ. 895 (1961).

¹⁷ E. Fairstein, Oak Ridge National Lab. Report No. ORNL-3348, 1962 (unpublished).

The coincidence unit used zero cross-over pick off circuits with integral pulse-height discriminators designed by Chase.¹⁸ A coincidence resolving time of 100 nsec was used.

Output pulses from the linear amplifiers were sent through delay lines, electronically added, and displayed on a single beam oscilloscope. A linear gate in the anticoincidence channel allowed the output of the anticoincidence detector to be displayed for 6 μ sec.

The requirement for an oscilloscope trigger was a B1-B2-A or B1-B2-C coincidence unaccompanied by a pulse from the anticoincidence shield. Discrimination levels were about 150 keV in each of the inner detector counters and 250 keV in the anticoincidence shield.

For calibration of the main detector by cosmic rays, the oscilloscope was triggered whenever an energy deposit of more than 100 MeV occurred in the anticoincidence detector. (A minimum-ionizing particle passing completely through the anticoincidence detector would deposit a minimum of 195 MeV).

Source Preparation

Sources were prepared from Nd_2O_3 enriched to 92.5% Nd^{150} obtained on loan from the Oak Ridge National Laboratory. Spectrographic analysis of the Nd_2O_3 sample furnished by Oak Ridge showed its chemical purity to be greater than 98.5%, with definite trace amounts of Ca, Mg, La, Pr, and Sm present. No attempt was made at further chemical purification. A 300-mg sample of the Nd_2O_3 was checked for β activity with a small plastic scintillator surrounded by a NaI(Tl) anticoincidence shield. A count rate of less than 0.1 count/min above 0.6 MeV was obtained.¹⁹

The double beta decay sources consisted of four 20.5-cm-square bags made from 1-mil Mylar, each containing

¹⁸ R. L. Chase, Rev. Sci. Instr. 31, 945 (1960).

¹⁹ This activity was not contributed to by the decay of Nd^{144} since the samples were contained in Mylar thick enough to totally absorb 2-MeV α particles.

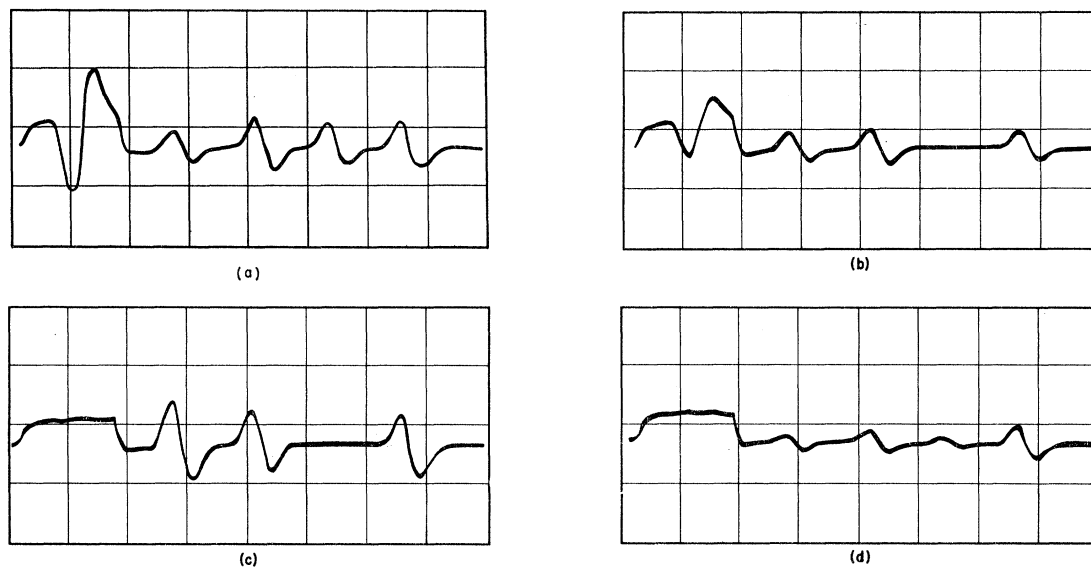


FIG. 5. Typical oscilloscope traces. Pulse order from left to right: Anticoincidence pulse (on pedestal), A , $B1$, C , and $B2$ pulses from main detector. (a) Calibration pulses from pulse generator. Approximate scale is 250 keV/division for anticoincidence pulse, 1 MeV/division for main detector pulses. (b) Anticoincided A , B event. (c) A , B event with no anticoincidence. (d) A , B , C event with no anticoincidence.

13.5 g of Nd_2O_3 . The Nd_2O_3 for each bag was first ground to a fine powder and mixed with 7 cc of distilled water and 0.5 cc of Kodak "Photo-Flo 200" solution, making a thick paste. This was then spread into a uniform layer inside the Mylar bag, and the bag was sealed with a heat-sensitive adhesive tape.²⁰ Most of the water was allowed to evaporate through the Mylar before the sources were placed in the detector. The four sources contained a total of (42.9 ± 0.2) g of Nd^{150} .

Background measurements were made using dummy sources of approximately the same mass as the Nd^{150} sources but containing sheets of Mylar. The same amounts of water and Photo-Flo were placed in the dummy sources as were used in the Nd^{150} sources. The use of another Nd isotope would have been preferred, but large amounts were not available. Natural Nd was considered, but available samples were found to contain measurable amounts of β activity.

The experimental data were obtained in three series of runs of approximately equal length. For the first series, four Nd^{150} sources were placed side by side between detectors B and C and four dummy sources were placed between detectors A and B . In the second series, the positions of the Nd^{150} and dummy sources were interchanged; the third series of runs was made with dummy sources located between both pairs of detectors.

3. DATA ANALYSIS

The data were obtained as photographs of oscilloscope traces, examples of which are shown in Fig. 5. The film

²⁰ "Schjeldbond" Thermoplastic Adhesive manufactured by the Schjeldahl Company, Northfield, Minnesota.

was read on a semiautomatic reading machine which yielded punched paper tape containing Cartesian coordinates of positions on each of the five pulses. Suitable calibration pulses were photographed and measured for each run. Data from the paper tape were read and processed by a digital computer and the results stored on magnetic tape.

Processing of the double beta-decay data consisted of searching the recorded data for events that produced pulses in both phototubes viewing the center scintillator in the main detector ($B1$ and $B2$ signals) and a pulse from the top (A signal) or bottom (C signal) scintillator unaccompanied by an anticoincidence (D signal) pulse, with pulse-height requirements being imposed on each pulse. An event would also be accepted if it met all requirements except that both A and C pulses were present provided that either the A or C pulse was less than an acceptable "feedthrough" level. All of the requirements on the sizes of pulses for an acceptable event could be changed during subsequent analysis.

During the analysis, pulse-height spectra were accumulated and plotted for all pulses from the three scintillators in the main detector that met the requirements for an acceptable event. Also the pulse-height correlations, defined in the sense of cross correlations between samples,²¹ were calculated for the main detector signals.

During the data runs the pulse-height selectors on the coincidence unit were set to accept pulses greater than 150 keV to 200 keV from the main detector, and the

²¹ See, for example, Lyman G. Parratt, *Probability and Experimental Errors in Science* (John Wiley & Sons, Inc., New York 1961), p. 140.

TABLE II. Results of data analysis.

Run No.	Events analyzed	Run time ^b (h)	<i>A, B</i> rate (counts/h)	<i>A, B</i> correlation	<i>B, C</i> rate (counts/h)	<i>B, C</i> correlation
A. First series of runs ^a : Nd ¹⁵⁰ source between detectors <i>B</i> and <i>C</i>						
810	1396	4.07	80.2 ±4.4	+0.005	39.1 ±3.1	-0.125
811	2860	8.57	73.0 ±2.9	-0.150	38.6 ±2.1	-0.001
813	2905	8.94	70.8 ±2.8	-0.176	34.9 ±2.0	-0.030
814	1491	4.38	82.4 ±4.3	-0.197	31.9 ±2.7	-0.028
817	1469	2.86	78.4 ±5.2	-0.235	39.2 ±3.7	+0.058
818	1451	3.28	90.8 ±5.3	-0.283	49.4 ±3.9	-0.015
826	2993	14.85	75.0 ±2.2	-0.138	35.8 ±1.5	-0.038
827	1494	7.27	73.8 ±3.2	-0.125	32.9 ±2.1	-0.048
903	1100	4.35	98.2 ±4.8	-0.160	38.8 ±3.0	-0.018
904	1467	7.21	76.0 ±3.2	-0.173	28.0 ±2.0	-0.099
909	1488	7.21	76.3 ±3.3	-0.169	37.3 ±2.3	+0.010
910	2877	13.96	71.3 ±2.3	-0.113	35.6 ±1.6	-0.007
916	1081	5.30	69.1 ±3.6	-0.133	41.3 ±2.8	-0.160
917	2909	14.37	69.5 ±2.2	-0.145	32.8 ±1.5	-0.091
921	1598	7.78	73.6 ±3.1	-0.114	35.0 ±2.1	+0.006
922	3120	15.01	74.2 ±2.2	-0.176	32.8 ±1.5	-0.079
All	31 699	129.40 (123.95) ^c	74.88±0.76 (78.2 ±0.8) ^c	-0.144	35.38±0.54 (36.9 ±0.5) ^c	-0.049
B. Second series of runs ^a : Nd ¹⁵⁰ source between detectors <i>A</i> and <i>B</i> .						
1111	3173	12.12	77.5 ±2.5	-0.031	40.2 ±1.8	-0.109
1112	3190	11.51	81.7 ±2.6	-0.055	36.2 ±1.7	-0.261
1116	3099	11.52	83.6 ±2.7	-0.047	39.6 ±1.9	-0.296
1117	3149	11.74	74.3 ±2.5	-0.070	34.6 ±1.7	-0.117
1119	3193	13.19	78.0 ±2.4	-0.057	41.4 ±1.8	-0.170
1123	1597	6.39	75.7 ±3.5	-0.096	37.3 ±2.4	-0.175
1124	3195	12.92	80.0 ±2.5	-0.031	42.2 ±1.8	-0.189
1125	1494	5.90	76.8 ±3.6	-0.097	35.9 ±2.5	-0.136
1130	3168	12.76	77.1 ±2.5	-0.042	40.8 ±1.8	-0.083
1201	1599	6.44	71.4 ±3.3	-0.056	47.6 ±2.7	-0.191
1207	3201	13.31	80.0 ±2.5	-0.029	45.9 ±1.9	-0.212
1210	1599	6.67	79.6 ±3.4	-0.095	42.6 ±2.5	-0.218
All	31 657	125.16 (119.89) ^c	78.43±0.79 (81.9 ±0.8) ^c	-0.047	40.39±0.56 (42.2 ±0.6) ^c	-0.181
C. Third series of runs ^a : No Nd ¹⁵⁰ source.						
120	1586	8.56	71.7 ±2.9	-0.101	22.9 ±1.6	-0.011
121	1270	6.58	70.9 ±3.3	-0.128	17.8 ±1.6	-0.138
128	3181	16.16	66.6 ±2.0	-0.131	18.7 ±1.1	-0.110
129	1583	8.29	68.8 ±2.9	-0.087	32.3 ±2.0	-0.045
201	1599	8.18	62.5 ±2.8	-0.105	22.5 ±1.7	-0.072
202	1599	8.33	64.1 ±2.8	-0.114	20.4 ±1.6	-0.206
203	3192	16.59	65.3 ±2.0	-0.085	27.1 ±1.3	-0.099
204	3198	16.52	68.7 ±2.0	-0.117	26.6 ±1.3	-0.154
210	3195	16.24	67.9 ±2.0	-0.086	28.0 ±1.3	-0.060
All	20 401	105.45 (101.93) ^c	67.18±0.80 (69.6 ±0.8) ^c	-0.103	24.49±0.48 (25.4 ±0.5) ^c	-0.104

^a Pulse height restrictions: anticoincidence pulse ≤50 keV, coincidence pulses ≥300 keV, feedthrough pulse ≤100 keV.

^b Run times corrected for loss of data due to bad spots on film, paper tape punch errors, etc.

^c Corrected for camera dead time of 0.6 sec/event.

anticoincidence level was chosen as about 250 keV. Test runs, in which the coincidence circuit was triggered by a pulse generator, showed that the anticoincidence channel on the film was free enough of accidental pulses to allow an anticoincidence level of 50 keV to be imposed during the data analysis with less than 1% loss of sensitive time. It was found that the smallest pulses from the main detector outputs that could be read with any degree of certainty were between 70 and 100 keV, therefore the *A* or *C* feedthrough level was set at 100 keV during the final data analysis. The coincidence acceptance levels were set at 300 keV for the final data analy-

sis in order to minimize the effects of variations in pulse-height selector settings for the three series of runs.

Results of the final analysis of each run are summarized in Table II. The errors quoted are one standard deviation in the total count. The *A, B* count rates and pulse-height correlations are for *A, B1, B2*, (no *D*) events with no pulse in the *C* channel greater than 100 keV, and the *B, C* count rates and correlations are for *B1, C, B2*, (no *D*) events with no *A*-channel pulse greater than 100 keV.

The negative pulse-height correlations are consistent both with double-beta-decay events and with a γ -ray

background, since in both cases a high-energy electron in one detector would tend to be accompanied by a lower energy electron in an adjacent detector. Possible sources of background events are discussed below.

4. DETECTION EFFICIENCY

In order to estimate the efficiency of the detectors for double beta decay events, it is necessary to assume energy and angular distribution for the decay electrons. The distributions used were those calculated by Primakoff and Rosen.⁵

For the two-neutrino decay mode, the probability of one decay electron having kinetic energy between E_1 and E_1+dE_1 and the other having kinetic energy between E_2 and E_2+dE_2 is given by

$$P_2(E_1, E_2) dE_1 dE_2 \simeq \text{const}(E_0 - E_1 - E_2)^5 (E_1 + 1)^2 (E_2 + 1)^2 dE_1 dE_2, \quad (2)$$

subject to the condition that $E_1 + E_2 \leq E_0$, where E_0 is the kinetic-energy release of the double beta decay. Units are chosen such that $c = \hbar = m_e = 1$. The kinetic-energy distributions for either of the decay electrons and for the sum of the kinetic energies of both electrons are obtained by integrating Eq. (2) over the appropriate energies, giving

$$P_2'(E_1) dE_1 \simeq \text{const}(E_0 - E_1)^6 (E_1 + 1)^2 \times [(E_0 - E_1)^2 + 8(E_0 - E_1) + 28] dE_1 \quad (3)$$

$$C_0(E_1, E_0 - E_1, \theta) \times \frac{1}{2} \sin\theta d\theta \simeq \left[1 - \frac{E_1^2 + E_2^2 + 4E_1 + 4E_2 + 2(E_1 E_2 + 1)}{(E_1^2 + E_2^2 + 2E_1 + 2E_2)(E_1 + 1)(E_2 + 1) + 2(E_1 + 2E_1)(E_2 + 2E_2)} \right] \times \frac{1}{2} \sin\theta d\theta. \quad (7)$$

The single electron kinetic-energy distributions given by Eqs. (3) and (6) are plotted in the upper part of Fig. 6. The sum kinetic-energy distribution given by Eq. (4) is shown in the upper part of Fig. 7.

The decay energy E_0 must be determined from mass spectrographic data. A recent direct measurement²³ of the Nd^{150} - Sm^{150} mass difference gives $E_0 = (3.384 \pm 0.004)$ MeV for the double beta decay of Nd^{150} . This value is significantly less than the previously obtained value of (3.65 ± 0.10) MeV,²⁴ but in agreement with the value of (3.39 ± 0.02) MeV obtained from the adjusted relative atomic mass table of Mattauch *et al.*²⁵ The value of 3.4 MeV was used for calculational purposes.

²³ S. P. Rosen, Proc. Phys. Soc. (London) **74**, 350 (1959).

²⁴ W. McLatchie, R. C. Barber, H. E. Duckworth, and P. Van Rookhuyzen, Phys. Letters **10**, 330 (1964).

²⁵ W. H. Johnson, Jr., and A. O. C. Nier, Phys. Rev. **105**, 1014 (1957).

²⁶ J. H. E. Mattauch, W. Thiele, and A. H. Wapstra, Nucl. Phys. **67**, 1 (1965).

for the single electron kinetic-energy distribution, and

$$P_2''(E) dE \simeq \text{const}(E_0 - E)^5 \times (E^4 + 10E^3 + 40E^2 + 60E + 30) E dE, \quad (4)$$

with $E = E_1 + E_2 \leq E_0$, for the sum kinetic-energy distribution. The angular correlation function is given by

$$C_2(E_1, E_2, \theta) \times \frac{1}{2} \sin\theta d\theta \simeq [1 - \mathbf{p}_1 \cdot \mathbf{p}_2 / (E_1 + 1)(E_2 + 1)] \times \frac{1}{2} \sin\theta d\theta, \quad (5)$$

where \mathbf{p}_1 and \mathbf{p}_2 are the electron momenta, and θ is the angle between the two electron momenta. The quantities $C_2(E_1, E_2, \theta) \times \frac{1}{2} \sin\theta d\theta$ and $P(E_1, E_2) dE_1 dE_2$ are sensitive to the approximations made for the matrix elements of the "intermediate" nucleus lying between the parent and final nuclei. However, Rosen has shown that the shape of the sum kinetic-energy distribution, $P_2''(E) dE$, is fairly independent of this and other approximations made in the calculation.²²

For the neutrinoless mode of decay, all of the decay energy is shared by the two electrons with a single electron kinetic-energy probability distribution given by

$$P_0'(E_1) dE_1 \simeq \text{const}(E_1 + 1)^2 \times (E_0 - E_1 + 1)^2 A(E_1, E_0 - E_1) dE_1, \quad (6)$$

where

$$A(E_1, E_2) \simeq \text{const} [p_1^2 + p_2^2 + 2p_1^2 p_2^2 / (E_1 + 1)(E_2 + 1)].$$

The sum energy distribution is, of course, a delta function at E_0 . The angular correlation function is given by

Other factors to be considered in calculating the detection efficiency are: (1) finite low-energy cutoff, (2) detector resolution, (3) energy loss and scattering in the source, and (4) electrons passing into a second plastic scintillator sheet or the anticoincidence detector. The effects of (4) will be more important for the neutrinoless decay mode since the average energy of the decay electrons is greater.

The primary effect of detector resolution is the introduction of energy uncertainty in the pulse-height discrimination levels. What effect this has on the detection efficiency depends upon the electron energy probability distributions as well as the width of the detector resolution function. The resolution function was assumed to be a normal distribution centered about the "true" electron energy E with a standard deviation proportional to \sqrt{E} .

A relation for the approximate energy loss per unit thickness of absorber can be obtained by differentiating one of the many empirical range-energy relations for

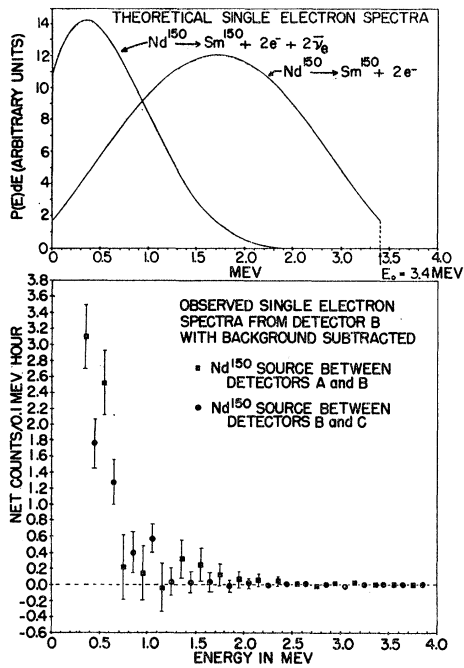


FIG. 6. Upper: Theoretical single electron spectra for two-neutrino and neutrinoless double beta decay. Lower: Observed single electron spectra associated with the two Nd^{150} source positions.

monoenergetic electrons. The relation chosen for this purpose was that of Katz and Penfold.²⁶

A "Monte-Carlo" method was used to calculate the detection efficiencies for both possible decay modes as a function of the low-energy cutoff E_d imposed on each detector, the allowed feedthrough energy E_f , and the low-energy cutoff imposed on the sum spectrum E_s , where $E_s \geq 2E_d$. The results of the calculations for $E_d=0.3$ MeV, $E_f=0.1$ MeV, and various values of E_s are tabulated in Table III.

5. RESULTS

The pulse-height spectra obtained from detector B (the sum of signals B1 and B2) associated with the two Nd^{150} source positions are shown in the lower part of

TABLE III. Calculated detection efficiencies.^a

Two-neutrino decay mode		Neutrinoless decay mode	
E_s (MeV)	Det. eff. (percent)	E_s (MeV)	Det. eff. (percent)
0.8	20	2.8	10
1.0	19	3.0	8
1.3	14	3.2	6
2.0	4	3.4	4
2.3	2	3.6	2

^a An energy deposit of ≤ 0.1 MeV in a third plastic scintillator or < 50 keV in the anticoincidence detector is allowed. The low-energy cutoff imposed on each main detector is 0.3 MeV. E_s is the low-energy cutoff imposed on the coincidence spectrum.

²⁶ L. Katz and A. S. Penfold, Rev. Mod. Phys. 24, 28 (1952).

Fig. 6. The background spectrum used in the subtraction was that obtained during the third series of runs with only the dummy sources in the main detector. The background spectra obtained in the first two series of runs showed evidence of having been affected by the presence of a beta emitter in the Nd_2O_3 . Coincidence spectra associated with the two source positions are shown in the lower part of Fig. 7, with the high-energy region shown in more detail in Fig. 8. The observed coincidence count rates are consistent with a lower limit of 3×10^{17} years for the half-life of the decay $Nd^{150} \rightarrow Sm^{150} + 2e^- + 2\bar{\nu}_e$, and a lower limit of 5×10^{18} years for the half-life of the decay $Nd^{150} \rightarrow Sm^{150} + 2e^-$. The spectra that would be expected for these two decay half-lives based on the detection efficiency calculations outlined above are also shown in Figs. 7 and 8.

Sources of Background

The most probable cause of background events would appear to be the Compton scattering of γ rays in one of the plastic scintillators in the main detector giving rise to an electron able to penetrate into an adjacent scintillator. A measurement of the coincidence count rates between adjacent scintillators and between the top and bottom scintillators indicated that successive Compton scatterings of a single γ ray in adjacent scintillators accounted for no more than one-third of the observed background count.

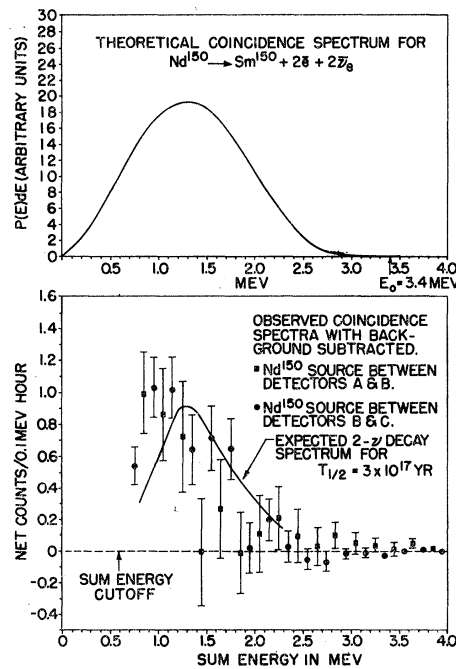
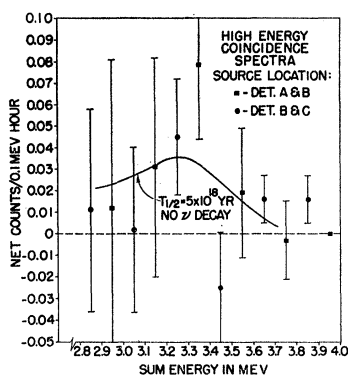


FIG. 7. Upper: Theoretical coincidence, or sum, electron spectra for two-neutrino double beta decay. Lower: Observed coincidence spectra associated with the two Nd^{150} source positions. The solid curve is the spectrum expected for a two-neutrino decay mode half-life of 3×10^{17} yr taking into account the detector efficiency as a function of electron energy.

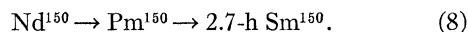
FIG. 8. High-energy portion of the observed coincidence spectra shown in greater detail. The solid curve is the spectrum expected for a neutrinoless decay mode half-life of 5×10^{18} yr taking into account the detector efficiency.



Coincidence pulse-height spectra obtained from each of the three series of runs all showed a definite peak in the vicinity of 1.5 MeV. Coincidence spectra obtained with Co^{60} and K^{40} sources located in the anticoincidence tank directly above the main detector failed to show any peaks in this energy region. This would indicate that γ rays with energies greater than 1.5 MeV, perhaps from ThC'' , accounted for a large part of the observed background. This is rather surprising in view of the fact that the count rate observed from the anticoincidence detector between 2.2 and 2.8 MeV was almost an order of magnitude lower than the rate between 1.2 and 1.8 MeV, as can be seen from Fig. 3.

The anticoincidence factor, i.e., the ratio of the coincident count rate observed with the anticoincidence channel inactive to the count rate with active anticoincidence, was found to be 1.8 with the anticoincidence discrimination level set at 250 keV and the main detector discrimination levels set at 160 keV. Using the same energy discrimination levels, the anticoincidence factor was found to be 6.8 with the Co^{60} source present and 3.1 with the K^{40} source. This would indicate that at least part of the background was due to a small amount of radioactive contamination of the main detector itself, which might also account in part for the difference observed between the *A, B* and *B, C* coincidence rates (see Table II).

Figure 9 shows the net coincidence spectrum from detectors *B* and *C* associated with the Nd^{150} source located between detectors *A* and *B*. A similar spectrum was obtained from detectors *A* and *B* associated with the source between detectors *B* and *C*. A possible explanation for this observed spectrum would be that it was due to a β^- emitter with an end point energy of ~ 2.5 to 3 MeV contained within the Nd_2O_3 . The cutoff in the spectrum at ~ 1.5 MeV corresponds to the minimum energy electron that could penetrate scintillator *B* (0.46 cm thick) and deposit enough energy in scintillator *C* to trigger the coincidence pulse-height discriminator. An interesting speculation as to the source of this decay would be to attribute it to the 2.7-h decay of Pm^{150} resulting from the β^- decay of Nd^{150} :



Pm^{150} β^- decays with an end point energy of 3.05 MeV (20%) or 2.01 MeV (80%).²⁷ The Nd^{150} - Pm^{150} mass difference is given by Mattauch *et al.*²⁵ as (-40 ± 60) keV which does not rule out the possibility of a low-energy β^- decay of Nd^{150} . However, McLatchie *et al.*²³ conclude that the above mass difference is (-76 ± 30) MeV and hence that Nd^{150} is stable against β^- decay. No information appears to be available on the Nd^{150} - Pr^{150} mass difference. Assuming that the observed spectrum is the result of the single beta decay of Nd^{150} , then the observed count rate allows a lower limit of $\sim 10^{17}$ yr to be placed on the half-life of such a decay. The previous limit set on the half-life of the single beta decay of Nd^{150} was $\sim 10^{16}$ yr.²⁸

The Nd_2O_3 used as the Nd^{150} source was known from spectrographic analysis to contain a trace of La amounting to less than 0.04%. La^{138} undergoes electron capture and β^- decay with a half-life of 1.1×10^{11} yr., emitting 0.21-MeV β^- particles and γ rays of 0.8 and 1.4 MeV.²⁷ This could account for no more than about 5 γ rays per hour being produced within the Nd_2O_3 source itself. Even extremely minute amounts of K^{40} or any of the Ra or Th series γ emitter present in the Nd_2O_3 or in any of the materials in the immediate vicinity of the plastic scintillators could produce a significant number of background events. The presence of α -particle emitters would appear to present no problem because of the extremely short range of α 's for any reasonable energy.

6. CONCLUSIONS

In view of the uncertainties involved in determining and eliminating the effects of background, the half-lives quoted above should be considered only as lower limits imposed by the experimental conditions. On the question of the neutrinoless decay mode, the results obtained are certainly not conclusive enough to rule out the possibility that this mode of decay might occur in conjunction

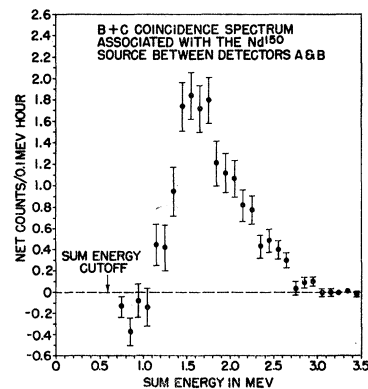


FIG. 9. "Feed-through" coincidence spectrum associated with the source between detectors *A* and *B*.

²⁷ D. Strominger, J. M. Hollander, and G. T. Seaborg, *Rev. Mod. Phys.* **30**, 585 (1958).

²⁸ D. Dixon and A. McNair, *Phil. Mag.* **45**, 1099 (1954).

with the two-neutrino decay as has been suggested by Greuling and Whitten.⁷

ACKNOWLEDGMENTS

The author wishes to express his gratitude to Professor F. Reines for suggesting this work, and to Pro-

fessor T. L. Jenkins for many valuable discussions and suggestions. Thanks are also due to A. A. Hruschka for supervising the mechanical design and construction of the anticoincidence detector, F. W. Dix and G. R. Smith for their help in collecting and analyzing the data, and to the Morton Salt Company for their gracious hospitality and help at their Fairport Harbor Mine.

M , N , and O Subshell Conversion Coefficients in ^{228}Th and ^{240}Pu

A. V. RAMAYYA, B. VAN NOOIJEN,* S. R. AMTEY,† AND J. H. HAMILTON

Vanderbilt University, ‡ Nashville, Tennessee

(Received 18 April 1966)

The M , N , and O subshell conversion coefficients of the 57.9-keV, $2^+ \rightarrow 0^+$ transition in ^{228}Th and the M and N subshell conversion coefficients of the 42.88-keV, $2^+ \rightarrow 0^+$ transition in ^{240}Pu have been measured with an iron-free double-focusing spectrometer. In the case of ^{228}Th , conversion coefficients obtained for the M_1 , M_2 , M_3 , M_4+M_5 , N_2 , N_3 , O_2 , and O_3 shells are 0.89 ± 0.22 , 19.1 ± 1.5 , 17.8 ± 1.3 , 0.55 ± 0.34 , 5.16 ± 0.46 , 4.97 ± 0.45 , 1.33 ± 0.22 , and 1.23 ± 0.20 , respectively. For the transition in ^{240}Pu , the conversion coefficients of the M_1 , M_2 , M_3 , N_1 , N_2 , N_3 and N_4+N_5 are 5.6 ± 2.1 , 107.2 ± 7.5 , 97.8 ± 7.0 , 2.9 ± 0.8 , 28.2 ± 2.9 , 28.7 ± 2.9 , and 2.3 ± 1.0 , respectively. Results from the M subshells are $(15 \pm 8)\%$ to $(85 \pm 45)\%$ higher than Rose's theoretical values after correcting for screening according to the semiempirical method of Chu and Perlman. The M -shell conversion-coefficient ratios for these $E2$ transitions agree with Rose's unscreened values within our experimental errors. This agreement suggests that the corrections due to screening for the different members in a particular shell are approximately the same.

1. INTRODUCTION

THE only available theoretical internal-conversion coefficients for the M subshells for wide Z ranges are those calculated by Rose¹ and these do not take into account the effects of screening and of the finite size of the nucleus. The finite nuclear size is generally of little importance; however, the effect of screening cannot be ignored at all. The calculated conversion coefficients are in disagreement with experimentally measured values for M subshells by factors as large as 3 (see, for example, Ref. 2). Recently Chu and Perlman² have introduced a semi-empirical method to correct the theoretical values for the screening effect. More recently Bhalla³ has calculated the M conversion coefficients of the $M4$ transition in ^{121m}Te using the non-relativistic potential calculated in the Hartree-Fock-Slater approximation. M , N , and O subshell conversion coefficients of the 57.9 keV $2^+ \rightarrow 0^+$ transition in ^{228}Th and M and N subshell conversion coefficients of the

42.88 keV $2^+ \rightarrow 0^+$ transition in ^{240}Pu have been measured to give a further test of the semi-empirical approach of Chu and Perlman,² as well as of new calculations as they become available.

2. EXPERIMENTAL METHODS

The ^{232}U isotope decays by α -emission to ^{228}Th , and the 57.9-keV first excited level is fed in 32% of the disintegrations. In the case of ^{244}Cm , which decays by α -emission to ^{240}Pu , 23% of the decays populate the 42.88-keV, first excited level. The sources used in this work were prepared by electro-deposition onto platinum foils and had areas of 16×1 mm². The source strengths were of the order of 10 μC , to keep the source thickness small.

These weak sources required long measuring periods of 24 to 48 h for each complete run. The measurements were made on an iron-free double-focusing spectrometer.⁴ The resolution of the spectrometer was set at 0.2%. The cutoff energy of the Geiger-Müller (G-M) counter window used was 5 keV; the dimensions of the G-M counter window were 16×1.5 mm². The L_3 line of each transition was also measured during each run to enable us to calculate the conversion coefficients relative to the theoretical L_3 conversion coefficient.

* On leave from the Technological University, Delft, Netherlands.

† On study leave from the Tata Institute of Fundamental Research, Bombay, India.

‡ Supported in part by a grant from the National Science Foundation, U.S.A.

¹ M. E. Rose, *Internal Conversion Coefficients* (North-Holland Publishing Company, Amsterdam, 1958).

² Y. Y. Chu and M. L. Perlman, *Phys. Rev.* **135**, B319 (1964).

³ C. P. Bhalla, *Internal Conversion Processes*, edited by J. H. Hamilton (Academic Press Inc., New York, 1966), p. 373.

⁴ Q. L. Bair, J. C. Nall, S. K. Haynes, and J. H. Hamilton, *Nucl. Instr. Methods* **16**, 275 (1962).